# Molecularly Imprinted Polymeric Nanospheres by Diblock Copolymer Self-Assembly

**Zhao Li,[†] Jianfu Ding,*[,†] Michael Day,[†] and Ye Tao[‡]**

*Institute for Chemical Process and Environmental Technology (ICPET) and Institute for Microstructural Sciences (IMS), National Research Council of Canada (NRC), 1200 Montreal Road, Ottawa, Ontario K1A 0R6, Canada*

*Received December 14, 2005; Revised Manuscript Received February 7, 2006*

ABSTRACT: Novel molecularly imprinted polymeric nanospheres (MIPNs) were prepared combining both molecular imprinting and block copolymer self-assembly techniques. A diblock copolymer, poly[(*tert*-butyl methacrylate)-*block*-(2-hydroxylethyl methacrylate)] (PtBMA-*b*-PHEMA), was synthesized by living free radical polymerization. Further postfunctionalization introduced 2-acrylamido-6-carboxylbutylamidopyridine (ACAP) and cross-linkable methacryloyl side groups into the polymer. The resulting final diblock copolymer was able to interact with 1-alkyluracil or 1-alkylthymine derivatives in chloroform to form triple hydrogen bonding complexes. Addition of cyclohexane, a block selective solvent, to this solution produced spherical micelles with uracil or thymine compounds embedded within the core, which was cross-linked in the solution in order to lock-in the MIP structures. The cross-linking has also made the core−shell structure of the micelle particles sufficiently stable for the subsequent extraction and rebinding process, which was confirmed by TEM and FTIR study. After cross-linking and extraction, these uniform nanospheres showed good dispersibility in organic solvents and demonstrated specific rebinding preponderancies to the target molecules of nucleotide bases, uracil, or thymine compounds. Comparing with the traditional bulk MIPs, these MIPNs demonstrated higher rebinding capacities and comparable size and shape selectivity.

## Introduction

Molecularly imprinted polymers (MIPs) are highly cross-linked porous polymers which are capable of specifically rebinding their target molecules. During the past decade these materials have attracted extensive attention because of their potential applications in a wide range of areas including chemical sensing, separation, drug delivery, and catalysis.[1] Traditionally, a MIP is prepared in the form of a microporous monolith, which was then crushed into a fine powder with irregular shapes and a wide size distribution of the particles. However, in many applications the shape and size of the MIP particles are of critical importance for their performance. Consequently, there is a trend to prepare MIPs with well-defined structures and small sizes in order to achieve higher affinity, selectivity, and rebinding capacity as well as better site accessibility. For example, MIP microspheres prepared by precipitation polymerization or using spherical silica templates have demonstrated better HPLC performance than those produced using a traditional method.[2] Similarly nanosized microgel MIP particles prepared by dispersion polymerization displayed improved selectivity for catalysis and molecular recognition capabilities.[3] In addition, single molecularly dendritic MIPs with regular spherical structures and much smaller sizes showed high selectivity to their targets.[4] Meanwhile, other MIPs with regular structures and small sizes such as nanotubes and nanowires also demonstrated an increased selectivity and high site accessibility.[5] All these observations clearly indicate that the size and regularity of the MIP particles are important parameters in determining the affinity, selectivity, capacity, and accessibility for recognizing target molecules. In this paper, a new approach for preparing MIPs with uniform spherical core−shell nanostructures by self-assembling a block copolymer in a selective solvent is proposed.

Recently, we reported on a method for preparing MIPs from functionalized cross-linkable copolymers,[6] The use of polymers instead of monomers in this approach facilitated the integration of MIPs into devices. On the basis of this work, the possibility for preparing well-dispersed MIP nanospheres using block copolymers has been explored. One of the most interesting properties of block copolymers is their self-assembly capability, which has been utilized to prepare various kinds of well-defined nanostructures such as spheres, rods, tubes, vesicles, and toroids.[7] Their nanoscopic sizes and uniform core−shell architectures make these polymeric materials very promising candidates in therapeutic and diagnostic applications.[8] The most attractive aspect of this approach is that the nanostructures can be fine-tuned by adjusting the block length, block properties (such as polarity and miscibility with selective solvent), block sequences, etc.[7]

Herein, we report a novel process for the preparation of uniform molecularly imprinted polymeric nanospheres (MIPNs, Scheme 1). A diblock copolymer was synthesized with one block containing functional groups for both hydrogen bond formation and cross-linking. After interacting with the template molecules to form hydrogen-bonding complexes, this block copolymer was allowed to self-assemble to form spherical micelles in a selective solvent. This desired structure was then locked in by cross-linking, and the cross-linked nanospheres were extracted to remove template molecules. The resulting MIPNs have demonstrated higher capacities than traditional bulk MIPs and comparable size and shape selectivity in rebinding the target molecules. The micelle structure of MIPNs with a highly cross-linked porous core surrounded by a highly soluble corona layer allows the particles to disperse in solvent easily.

[†] ICPET.
[‡] IMS.
* To whom correspondence should be addressed. E-mail: jianfu.ding@nrc-cnrc.gc.ca.

10.1021/ma0526793 CCC: $33.50 Published 2006 by the American Chemical Society
Published on Web 03/08/2006

**Scheme 1. Schematic Representation of the Preparation Process for Molecularly Imprinted Polymeric Nanospheres from Diblock Copolymer**

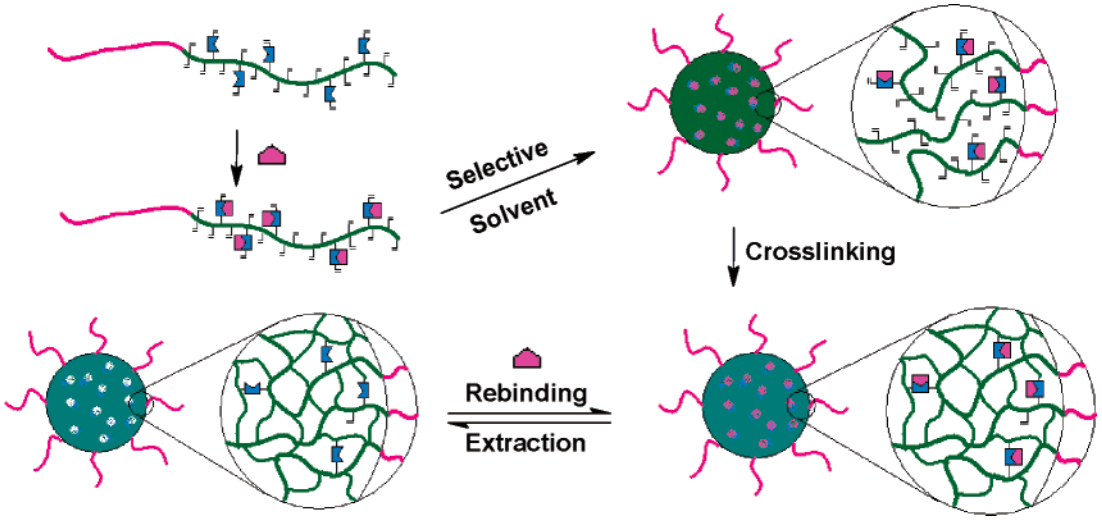


## Experimental Section

**General Methods.** *tert*-Butyl methacrylate (tBMA) and 2-(trimethylsilyloxy)ethyl methacrylate (HEMA-TMS) were obtained from Aldrich and purified by distillation under reduced pressure prior to use. Chloroform (stabilized with 0.75% ethanol) was purchased from BDH and used as received. Dichloromethane and triethylamine were distilled prior to use. 2,2′-Azobis(2,4-dimethylvaleronitrile) (V-65) was purchased from Wako Chemicals and used as received. All other reagents was purchased from Aldrich and used without further purification.

$^1$H NMR spectra were taken on a 400-MHz Varian Unity Inova spectrometer. FT-IR spectra were recorded on a Midac M1200-SP3 spectrophotometer using a diamond cell for solid samples and a KBr cell (0.1 mm thickness) for solution samples, from which the pure solvent background was subtracted. UV−vis absorption spectra were obtained on a Hewlett-Packard 8453 spectrophotometer. Molecular weights of the polymers were determined using gel permeation chromatograph (GPC) on a Waters model 515 HPLC equipped with $\mu$-Styragel columns using THF as eluant and calibrated using polystyrene standards. Transmission electron micrograph (TEM) images were taken on a Philips CM20 TEM with an UltraScan 1000 CCD camera made by Gatan.

**Synthesis of Uracil and Thymine Derivatives.** 1-Ethyluracil (EU), 1-butyluracil (BU), 1-ethylthymine (ET), and 1-butylthymine (BT) were synthesized according to a reported method.[9] 1,3-Dimethylthymine (DMT) was prepared by reacting thymine with iodomethane in the presence of $K_2CO_3$. All these compounds were purified by column chromatography and characterized with $^1$H NMR.

**Synthesis of 2-Acrylamido-6-carboxylbutylamidopyridine (ACAP).** A solution of acryloyl chloride (9.05 g, 0.10 mol) in 20 mL of dioxane was added dropwise with vigorous stirring to a solution of 2,6-diaminopyridine (22.0 g, 0.20 mol) in 100 mL of dioxane. The temperature was maintained at 25−30 °C using an ice/water bath. After reaction for 3 h, the solution was filtered to remove the solid, and the solvent was evaporated under reduced pressure using a rotary evaporator. The resulting oily residue was crystallized upon cooling to give 6.5 g (yield 40%) of crude product of 2-acrylamido-6-aminopyridine. $^1$H NMR ($CDCl_3$): 7.68 (1H, br, NH), 7.63 (1H, d, py), 7.48 (1H, t, py), 6.44 (1H, d, $=CH_2$, trans), 6.26 (1H, q, $=CH$), 6.26 (1H, d, py), 5.77 (1H, d, $=CH_2$, cis), 4.30 (2H, br, $-NH_2$).

This crude product (3.26 g, 0.02 mol) was then mixed with succinic anhydride (3.0 g, 0.03 mol) in 100 mL of dioxane. The solution was stirred at 60 °C for 3 h and 90 °C for 2 h. The solvent was then evaporated, and the residual solid mixture was purified by recrystallization in THF/hexane (40/60, v/v) to give 4.0 g of white product (yield: 76%). $^1$H NMR (DMSO): 12.14 (1H, s, COOH), 10.31 (1H, s, NH), 10.11 (1H, s, NH), 7.73−7.85 (3H, py), 6.66 (1H, q, $=CH$), 6.32 (1H, d, $=CH_2$, trans), 5.79 (1H, d, $=CH_2$, cis), 2.66 (1H, t, $-CH_2$), 2.53 (1H, t, $-CH_2$).

**Synthesis of Diblock Copolymer, P*t*BMA-*b*-PHEMA.** P*t*BMA-*b*-PHEMA was prepared using a two-step ATRP reaction. First, P*t*BMA macroinitiator was prepared by ATRP using the following procedure: CuBr (123.0 mg, 0.857 mmol) was added into a 100 mL round-bottom flask. The flask was sealed with a rubber septum, evacuated, and refilled with nitrogen three times. The degassed monomer, *t*BMA (11.2 mL, 68.8 mmol), *N*,*N*,*N*,*N*,*N*-pentamethyldiethylenetriamine (PMDETA, 180 $\mu$L, 0.862 mmol), and methyl 2-bromopropionate (MBrP, 192 $\mu$L, 1.72 mmol) were then added using a syringe, and the mixture was stirred at 80 °C for 16 h. The resulting solution was diluted with 40 mL of tetrahydrofuran (THF) and was passed through a short neutral activated alumina column to remove the catalyst. The polymer solution was then precipitated into ice water, and the powder was collected by filtration and dried under vacuum: 7.8 g (yield: 80%). GPC: $M_n = 9.05 \times 10^3$, PDI = 1.29.

The resulting P*t*BMA macroinitiator (2.5 g) together with CuBr (37.7 mg, 0.263 mmol) was added into a 100 mL round-bottom flask, which was then sealed with a rubber septum and degassed. Dichlorobenzene (9.0 mL), the second monomer, HEMA-TMS (9.0 mL, 41.0 mmol), and PMDETA (55 $\mu$L, 0.263 mmol) were added. The solution was heated at 80 °C overnight for polymerization before THF (30 mL) was added to dilute the solution. After running through a short neutral activated alumina column, the resulting solution was mixed with 6 mL of HCl (6 N) and stirred for 1 h and then dropped into hexanes to precipitate the polymer. The collected polymer was dissolved in 40 mL of THF and precipitated in cool water (1 L) to give the purified copolymer of P*t*BMA-*b*-PHEMA. GPC: $M_n = 5.2 \times 10^4$, PDI = 1.47.

**Postfunctionalization of the Diblock Copolymer.** The above diblock copolymer (2.0 g, 11.0 mmol of $-OH$ groups) was dissolved in 7 mL of DMF in a flask, to which was added THF (16 mL), *N*,*N*′-dicyclohexylcarbodiimide (DCC, 0.63 g, 3.0 mmol), 4-(dimethylamino)pyridine (DMAP, 0.036 g, 0.30 mmol), and ACAP (0.804 g, 3.0 mmol). This solution was stirred overnight at room temperature. After being filtered, the solution was precipitated into cool water. The precipitated polymer was collected and dried under vacuum to give the ACAP attached polymer (2.2 g, yield: 86%).

The ACAP attached polymer (2.2 g) was dissolved in a mixture of dichloromethane (30 mL) and triethylamine (11.6 mL). Methylacrylic anhydride (MAAN, 12.4 mL) was added, and the solution was stirred at room temperature for 4 h. The resulting solution was then dropped into hexane, and the precipitate was collected and dried to give 2.3 g (84%) of the final diblock copolymer.

**Preparation of MIPNs.** The following procedure represents the typical synthesis of molecularly imprinted polymeric nanospheres with EU as the template (MIPN-EU). The final diblock copolymer (0.30 g) and EU (1.1 mmol, 5 equiv relative to ACAP units) were dissolved in 69 mL of chloroform, and then a block selective solvent, cyclohexane (CHx, 231 mL), was added slowly along the flask wall. The resulting two-layer solution was then shaken vigorously to ensure quick mixing, which allowed for producing a bluish turbid micelle solution. After being purged with $N_2$ for 0.5 h, the solution was added with a free radical initiator, V-65 (36 mg, 0.15 mmol), and stirred at 60 °C overnight to cross-link the micelles. The resulting solution was then concentrated and dialyzed in methanol/THF (1/1 v/v) for 24 h. The regenerated cellulose Spectra/Por* dialysis tubing with MWCO 12 000−14 000 was used for dialysis with the solvent (200 mL) being replaced for more than five times during the whole period. The quantitative removal of the template from the micelles was confirmed by UV measurement. The micelle solution was then concentrated to 2 mL and precipitated into ice water. The white powder was collected by filtration and dried under vacuum. MIPN using ET as template (MIPN-ET) was also prepared in the same manner. Nonimprinted polymeric nanosphere (NIPN) was similarly prepared but in the absence of the template molecule.

**Preparation of Traditional MIPs (tMIPs).** tMIPs were prepared by the copolymerization of a cross-linker and a functional monomer, 2,6-bis(acrylamido)pyridine, in the presence of the template. The following is a typical procedure for tMIP-EU: EU (0.140 g, 1.0 mmol), ethylene glycol dimethacrylate (EGDMA, 2.00 g, 10.0 mmol), and 2,6-bis(acrylamido)pyridine (0.215 g, 1.0 mmol), which was prepared according to a reported method,[10] were dissolved in 7.0 mL of chloroform. The initiator V-65 (25 mg, 0.10 mmol) was added, and the solution was purged with $N_2$ prior to being heated at 60 °C overnight. The resulting monolith was ground to fine powder with a mortar and pestle and extracted with a mixture of methanol/chloroform (20/80 v/v) in a Soxhlet extractor for 20 h and then dried under vacuum. A yellowish polymer powder (2.10 g) was obtained; yield: 95%. Using the similar procedure, tMIP-ET and tNIP were also prepared by the addition of ET as the template and without the addition of any template, respectively.

**Measurement of Binding Constants.** The binding constants of 1-alkyluracils or 1-alkylthymines to the ACAP groups in the copolymer or functional monomer were measured using a standard $^1$H NMR titration experiment in $CDCl_3$ solution. The data were analyzed using a nonlinear least-squares fit procedure as described in the literature.[9d]

**$^1$H NMR Study of the Rebinding Capacity.** The recognition capability of all the MIPNs and tMIPs in $CDCl_3$ was investigated by $^1$H NMR. Caffeine was added to the solution at a constant concentration (2.1 mM) as an internal standard for quantitative analysis. It showed no rebinding to MIPNs and tMIPs and no interfering with uracil or thymine derivatives in NMR measurement. A typical measurement involved preparing a series of solutions of the target compound with a set of specific concentrations. A defined amount of the MIP sample was then added to these solutions, which was stirred for 10 min for rebinding. It was found that 10 min is sufficient for the MIPs to reach rebinding equilibrium. The concentrations of the free target molecule in the solutions before and after the addition of MIPs were then deduced from $^1$H NMR spectra by comparing the integration intensities of the peaks from the target molecule and from caffeine. The measurement for each data point was repeated three times, and the average values and standard deviations were reported in Figure 9.

## Results and Discussion

**Polymer Synthesis.** Following the procedure outlined in Figures 1 and 2, P*t*BMA-*b*-PHEMA has been successfully synthesized by a successive atom transfer radical polymerization (ATRP).[12] 2-Acrylamido-6-carboxylbutylamidopyridine (ACAP) was synthesized by a two-step reaction of 2,6-diaminopyridine with the corresponding acid chloride and anhydride.[10] This compound was then reacted with P*t*BMA-*b*-PHEMA in a molar ratio of ACAP/HEMA = 0.3 at 22 °C for 16 h. The $^1$H NMR spectrum (Figure 3b) indicated that this procedure converted 20% of the hydroxyl groups in the HEMA block to ester groups. The residual hydroxyl groups were then further quantitatively reacted with methacrylic anhydride (MAAN) to introduce more cross-linkable groups into the polymer.[6] The success of these reactions was confirmed by $^1$H NMR spectra, as shown in Figure 3.

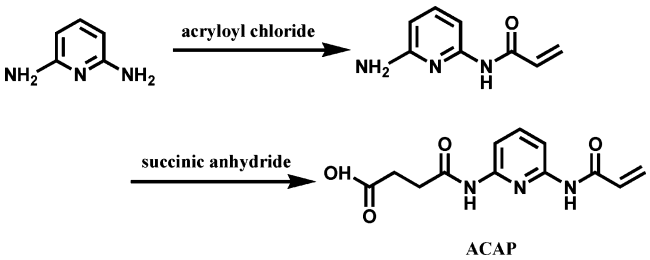


**Figure 1.** Synthetic approach for the preparation of compound ACAP.

**Micelle Formation and Cross-Linking**. The ACAP units in the final diblock copolymer can form a triple hydrogen bond with 1-alkyluracil or 1-alkylthymine derivatives (Figure 4), which has a binding constant of 380 ± 40 $M^{-1}$ in chloroform.[9] This interaction has been widely used to prepare MIPs with enhanced rebinding capacities and selectivity.[10] To prepare MIPNs, the final diblock copolymer was dissolved in chloroform along with a template. A block selective solvent, cyclohexane (CHx), was then added carefully along the flask wall onto the top of the chloroform solution without stirring. The resulting two-layer solution was then shaken vigorously to initiate rapid mixing and produced a bluish turbid micelle solution. In contrast, the slow addition of CHx to the chloroform solution with stirring resulted in the formation of precipitation of irregular aggregates. This indicates that the chain exchange between micelle particles is thermodynamically unfavorable under this condition, and the self-assembly process is kinetically controlled.[13] This feature greatly benefited the subsequent cross-linking of the micelle particles and prevented interfusion of particles during the cross-linking, which was confirmed by TEM studied as outlined below.

This self-assembly between the polymer and target molecules was studied by solution FT-IR. The FT-IR spectrum of pure BT in chloroform (Figure 5a) displayed a strong peak at 3400 $cm^{-1}$, which was assigned to N−H stretching. A similar N−H stretching peak was found at 3423 $cm^{-1}$ for the final diblock copolymer in chloroform and was attributed to free ACAP units (Figure 5b); meanwhile, a peak at 3350 $cm^{-1}$ was also observed and was assigned to the self-dimerized ACAP moieties. After mixing BT into the final polymer (Figure 5c), three new bands at 3278, 3219, and 3168 $cm^{-1}$ appeared, which belong to the triple hydrogen bond between ACAP and thymine as reported in the literature.[9a] Meanwhile, the N−H stretching peak at 3400 $cm^{-1}$ for free BT and the peaks at 3423 and 3350 $cm^{-1}$ for free and dimerized ACAP units decreased in intensity pronouncedly, indicating most of BT and ACAP moieties in solution combined to form triple hydrogen bonding complexes. The addition of the lower polarity solvent CHx into the solution significantly increased the relative intensity of the absorption bands of the triple hydrogen bonds in the region between 3168 and 3278 when compared with the N−H stretching band at 3400 $cm^{-1}$. This result indicated that the formation of the micelle particles by the addition of CHx enhanced the formation of the triple

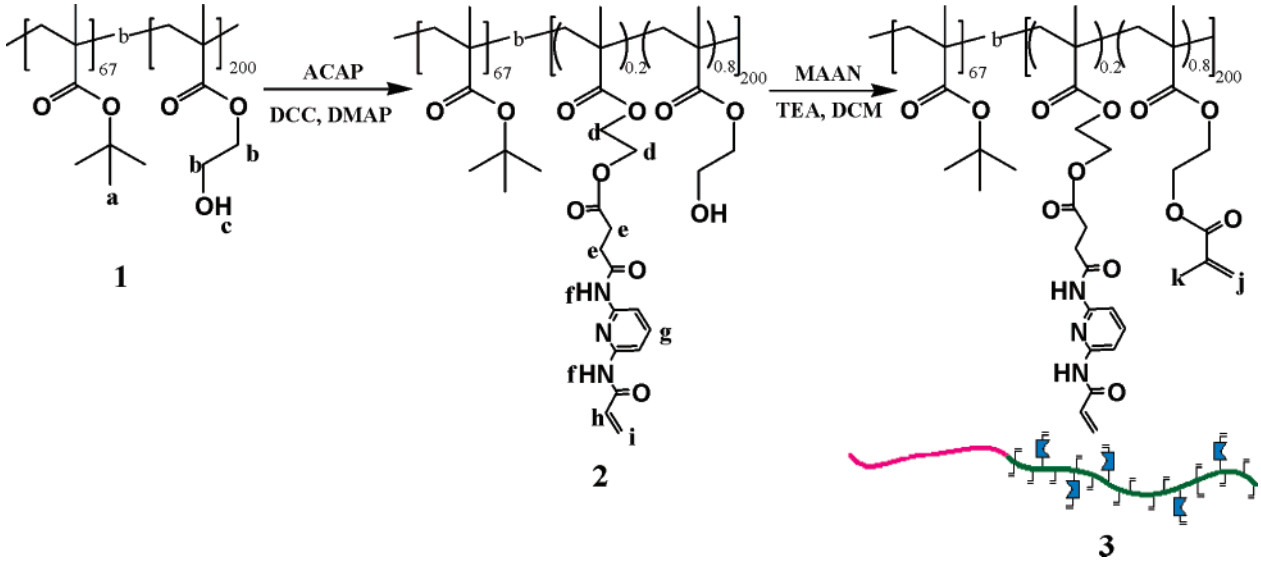


**Figure 2.** Synthetic route for the preparation of ACAP attached P*t*BMA-*b*-PHEMA(2) and the final diblock copolymer (3) from P*t*BMA-*b*-PHEMA (1).

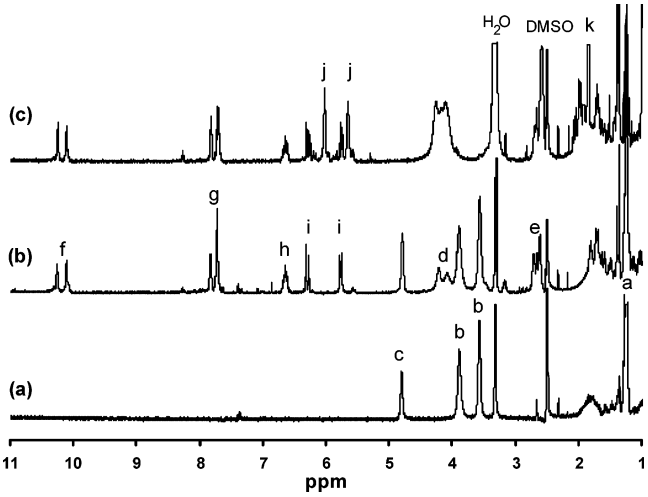


**Figure 3.** $^1$H NMR spectra of (a) P*t*BMA-*b*-PHEMA, (b) ACAP attached P*t*BMA-*b*-PHEMA, and (c) the final diblock copolymer in DMSO-$d_6$ (see Figure 2 for proton labels and polymer structures).

hydrogen bonds between BT and ACAP units. All these results suggest that during this self-assembling process (1) the formation of the triple hydrogen bonding complexes is predominant,[9a] (2) the equilibrium is shifted toward complex formation with the addition of CHx,[14] and (3) template molecule is indeed imbedded in the core of the micelles.

The formation of spherical micelles during the self-assembling process was confirmed by the TEM study. Figure 6a shows that the original micelle particles have a core size of about 50 nm. It was found that the dried sample of the cross-linked micelle particles could be easily redispersed into a solvent such as THF to form a tinted bluish solution, indicating that the cross-linked micelle particles were dispersed well in the solution. The TEM image (Figure 6b) demonstrated that the nanospherical structure of the micelle particles was retained after they was cross-linked, dried, and redissolved in a new solvent. This observation indicates that the cross-linking did not cause aggregation of the micelle particles, and the resulting highly cross-linked structure is strong enough to lock in the core−shell micelle structure. The formation of this highly cross-linked structure has also been confirmed by FT-IR (Figure 7). From this figure it can be clearly seen that the vibration of the carbon double bond at 1638 cm$^{-1}$ has completely disappeared after cross-linking, indicating a high conversion of the double bonds in the core of the micelle particles for the cross-linking process.[6] The high-resolution TEM image (Figure 6c) also confirmed the core−shell structures of the nanospheres. It should be noted that the particles for Figure 6b,c were deposited from THF solution. The particles have much higher swelling ratio in THF solution than in original micelle solution since THF is a much better solvent. Therefore, flatted spheres must form on the TEM grid from this solution. Consequently, larger core sizes appeared in Figure 6b,c than that from original micelle solution, as shown in Figure 6a. For the preparation of MIPN samples, the original cross-linked micelle solutions was concentrated and subjected to a dialysis using THF/methanol mixtures to remove the template molecules and impurities.[15] UV−vis measurement indicated that the template molecules were extracted quantitatively (data not shown).

**The Rebinding Ability of MIPNs and tMIPs.** For comparison purposes, traditional bulk MIPs (tMIPs) were prepared by a conventional method as outlined in the experimental part. Because of the smaller size and higher dispersibility of MIPNs in the solvent, the rebinding capability of MIPNs could not be studied by the conventional methods, including column chromatography and UV spectroscopy. It was therefore decided to use $^1$H NMR for obtaining this information using the line-broadening technique.[15] It was found that once the target molecule rebound to the MIP, its mobility was reduced dramatically due to the formation of the hydrogen bonding complex as well as its interaction with the surrounding of the recognition cavity. These effects broadened the NMR signals of the target molecule and even made them disappear completely.[16] Consequently, changes in the intensity of these signals can be used to detect and monitor the concentration of the free target molecule remaining in the solution during the rebinding. The reliability of this method was confirmed by comparing the rebinding result of tMIPs obtained by this $^1$H NMR approach with the result obtained by a conventional UV method (data not shown).

Figure 8 demonstrated the application of this technique to determine the rebinding capability of MIPN-EU to EU. The peaks from EU and the internal reference, caffeine, in $CDCl_3$

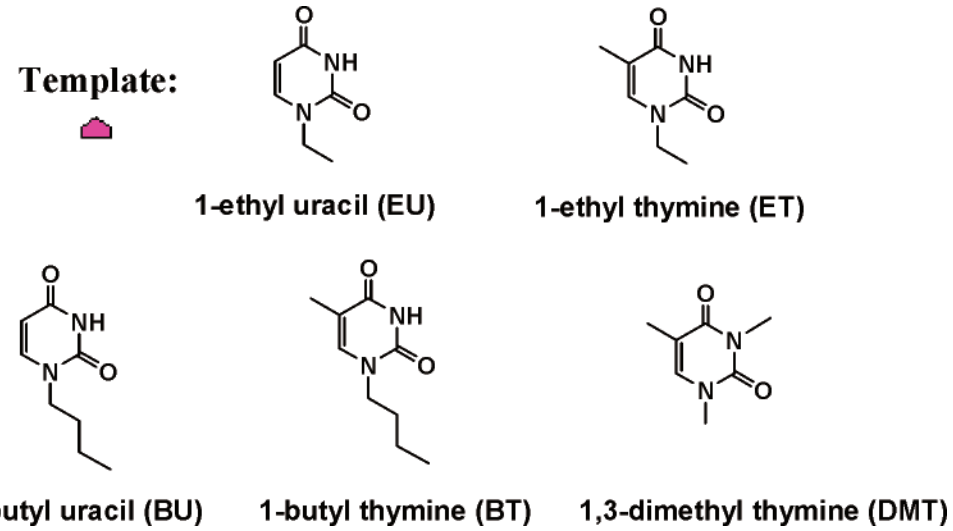


**Figure 4.** Molecular structures of templates and analytes used in this study.

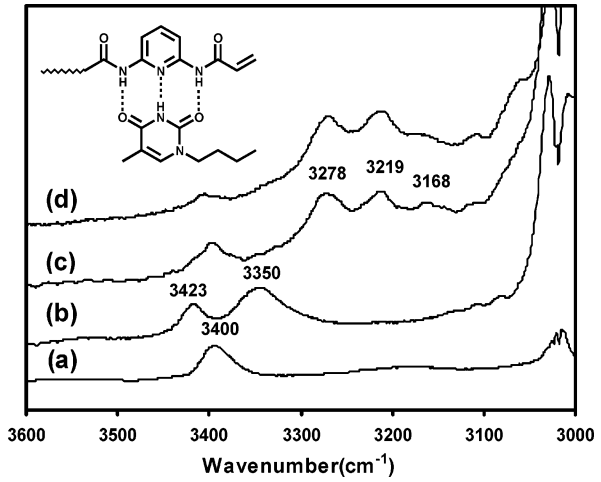


**Figure 5.** FT-IR spectra of (a) butylthymine (BT) in $CHCl_3$ (39 mM), (b) the final diblock copolymer in $CHCl_3$ (0.119 g/mL), (c) BT (74 mmol/L) and the final diblock copolymer (0.119 g/mL, 85 mmol/L ACAP units) in $CHCl_3$, and (d) micelle solution of BT (33 mmol/L) and diblock copolymer (0.053 g/mL, 38 mmol/L ACAP units) in a mixture of $CHCl_3$/cyclohexane (v/v = 1/3). The spectra were collected using the solvent as background.

were assigned as indicated in Figure 8a. With the addition of MIPN-EU into EU solution, the peaks from EU were broadened and their intensities decreased as the amount of MIPNs in the solution increased, while the signal from the internal reference, caffeine, remained unchanged. The variation of the free EU concentration in the solution could be obtained by comparing the integral intensity of peak d (3.80 ppm) with that of caffeine peak f at 3.98, 3.58, and 3.40 ppm.

Using this method, the rebinding isotherm for MIPNs, NIPNs, tMIPs, and tNIPs to the analytes (the structures are shown in Figure 4) was obtained and displayed in Figure 9. Both tMIPs and MIPNs showed much higher rebinding capacity than tNIPs and NIPNs, indicating the formation of the recognition cavities in MIPs. All MIPs showed negligible rebinding with DMT, confirming that the triple hydrogen bond between uracil or thymine and ACAP moieties played a very important role in the recognition for these MIP systems. Comparing to tMIPs, MIPNs showed higher rebinding capacity. The molar density of ACAP functional groups in MIPNs is about 1.6-fold that in tMIP ($7.1 \times 10^{-4}$ mol/g vs $4.5 \times 10^{-4}$ mol/g), while the rebinding capacity of MIPNs is 2.4-fold that of tMIPs at 8 mM template concentration (for example, MIPN-EU to EU, 450 $\mu$mol/g, vs tMIP-EU to EU, 190 $\mu$mol/g). This difference must be attributed to the nanoscopic core−shell structure of MIPNs; the recognition sites of MIPNs should be easy accessible to the target molecules due to the small and uniform size of the particles. Besides capacity, the MIPN-EU shows similar or slightly better selectivity than tMIP-EU toward the uracil or thymine derivatives. Figure 9a,c shows that the ratio of rebinding capacity of MIPN-EU to EU over ET or over BU at 8 mmol concentration was 1.33 or 1.12, while the ratio for tMIP-EU was only 1.19 or 1.10. Interestingly, when the template changed to ET, the resulting MIPN-ET (Figure 9d) still showed higher rebinding capacity to EU than to ET, while the bulk sample, tMIP-ET, showed a similar rebinding ability to EU and ET.

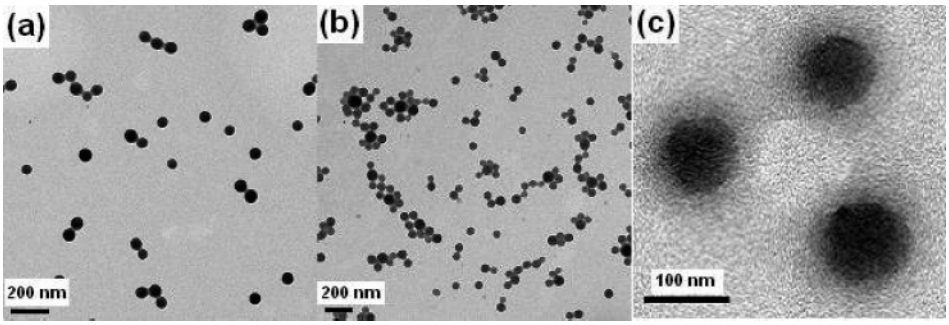


**Figure 6.** Transmission electron micrograph (TEM) image of (a) micelles formed from the final diblock copolymer in $CHCl_3$/cyclohexane (v/v = 23/77 at 1 mg/mL), (b) cross-linked micelle particles in tetrahydrofuran at 1 mg/mL, and (c) higher magnification of (b). All the samples were stained with $OsO_4$.

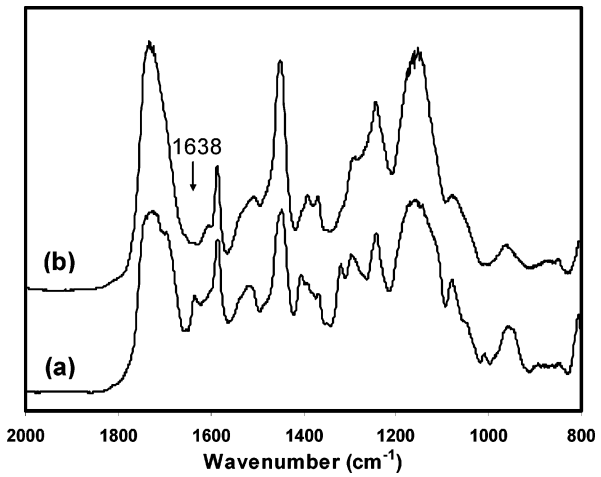


**Figure 7.** FT-IR spectra of (a) the final diblock copolymer and (b) cross-linked nanospheres.

Though this result seems to indicate that the selectivity of MIPN-ET to ET and EU based on their shape difference is poorer than tMIP-ET, it does not mean that MIPNs have worse shape selectivity than tMIPs. In this special case, both EU and ET have the same interaction with both MIPs and almost the same shape except one more methyl group in ET. The less bulky structure of EU makes it access the recognition cavity easier than ET. Therefore, the reason for this phenomenon is that the cavity created by ET has the right size to accommodate EU and is also be able to build up almost the same interaction with EU as with ET, in addition with the small and uniform core−shell structure of MIPNs ensures most cavities in the core easier accessible for EU. Actually similar or even higher shape selectivity of MIPNs than t-MIPs has been demonstrated in the above discussion by the higher ratio of the rebinding capacity of MIPN-EU to EU over to ET than that of tMIP-EU. A similar trend was also found for MIPN-EU in rebinding the target molecules with a more bulky group, BU and BT. MIPN-EU showed a higher rebinding capacity to BU than to BT.

Both MIPN-EU and tMIP-EU showed higher absorption to EU than BU, ET, and BT (Figure 9a), indicating a proper size exclusive effect in this system, which agrees well with other reported results.[10d] However, these two MIPs surprisingly showed higher rebinding capacity to BU than to ET, although ET is a relatively smaller molecule. This means that the selectivity of both nanospherical MIP and traditional MIP has a higher sensitivity to the shape selective effect than the size exclusive effect. This phenomenon must be caused by the high swelling ratio of the MIPs in the good solvent. The high swelling of the MIP particles might result in a slight expansion of the cavities and consequently made them able to accommodate analogous molecules with slightly lager size. Fortunately, this swelling effect is minor and only found for the MIP system with very small size difference between the template molecule and the target molecule. For the system with slightly increased difference in molecular size such as MIPs with ET as the template for rebinding BT and BU, the expected behavior has been observed, and both MIPN-ET and tMIP-ET displayed better rebinding capability to ET than to BT and even BU, demonstrating proper size exclusive effect of the recognition cavities in both MIPNs and tMIPs. To demonstrate this feature is extremely important for MIPN systems. It is believe that the uniform and small size of MIPN particles with a soluble corona layer will make the particles more swollen in the solution. These features in structures and swelling behavior offered advantages in enhancing rebinding capability of MIPNs, which will lead to desired higher accessibility to the most recognition cavities and result in high rebinding capacity. However, this swelling effect could also potentially deform the recognition cavities and cause the MIPNs to have reduced size selectivity. Therefore, it is a great advantage for our reported MIPN systems to remain a comparable size and shape selectivity as tMIP systems, in addition to having higher rebinding capacity due to the better accessibility to the recognition cavities than tMIP systems.

Although the difference of rebinding capacity of the MIPNs toward the different analytes is not so significant, it just reflects the reality of the very small difference in structure of these four analytes: EU, ET, BU, and BT. First, except for the small difference in the size and shape, the rebinding ability of the MIPs to these four analytes is mainly based on the same interaction, a strong triple hydrogen bond with ACAP unit. The difference of rebinding capacity became significant if we compared to an analogous target molecule, DMT, as shown in Figure 9b,d. This molecule has similar shape and size as the other four molecules, but only can form a single hydrogen bond with ACAP (see Figure 4 for structure). Second, the structures of these target molecules are very similar, and the difference of size and shape is very small. The only difference between

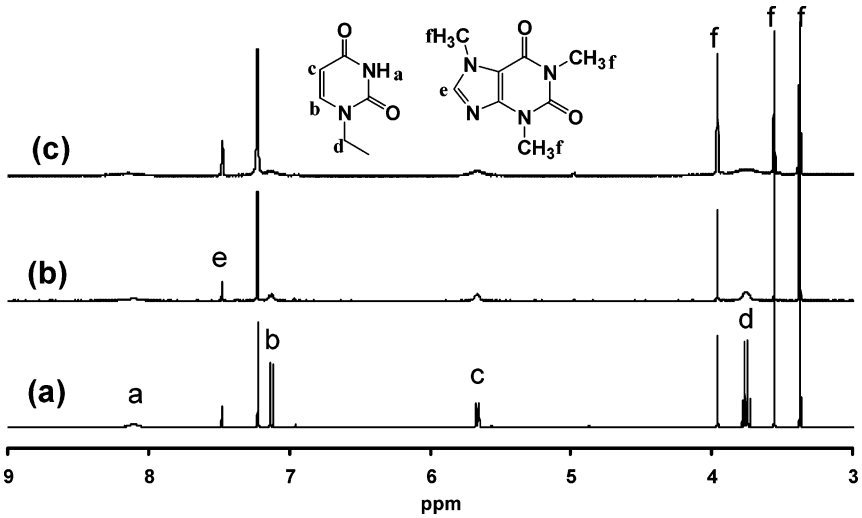


**Figure 8.** $^1$H NMR spectra of (a) EU (5.0 mM) and caffeine (2.1 mM) in 1.20 g of $CDCl_3$, (b) after 2.0 mg of MIPN-EU was added, and (c) after 8.0 mg of MIPN-EU was added.

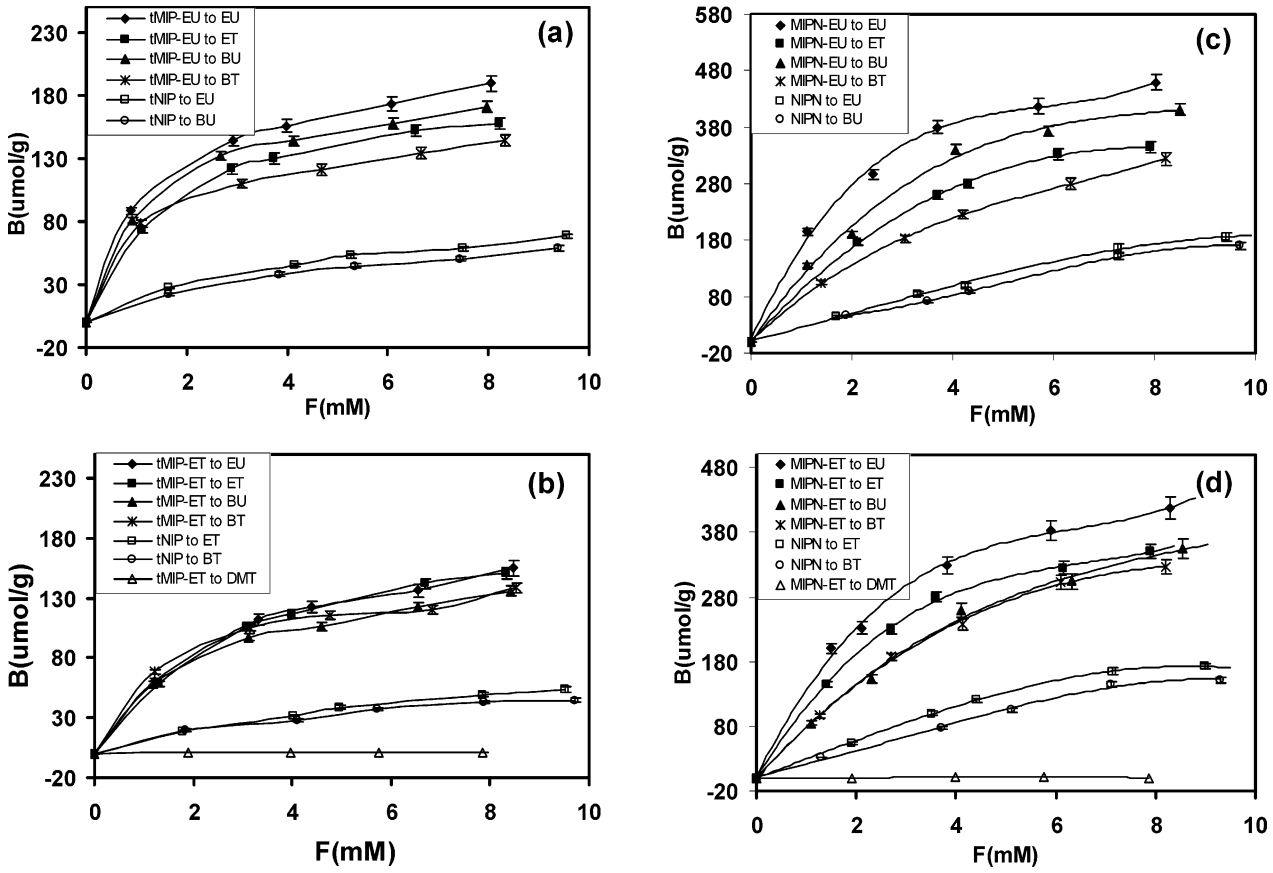


**Figure 9.** Rebinding isotherm to analytes of (a) tMIP-EU, (b) tMIP-ET, (c) MIPN-EU, and (d) MIPN-ET. The relevant rebinding isotherm for NIPs is also plotted.

EU and ET is that ET carries one more methyl group. On the basis of such small difference in structure, the results shown in Figure 9 already indicated a high sensitivity of the MIPNs to size and shape of the target molecules. Third, traditional bulk MIP systems always show a heterogeneous distribution in size and shape of particles, which cause some of the recognition cavities difficult to access.[17] Compared with traditional bulk MIPs, MIPNs have uniform nanosized core−shell morphology, good dispersibility in solvent, fast and complete removal of templates, high rebinding capacities, and comparable selectivity.

## Conclusions

A new approach has been proposed to prepare MIPNs combining molecularly imprinting and block copolymer self-assembly techniques. These MIPNs have uniform nanoscopic size, good dispersibility in solvent, and higher capacity and comparable selectivity with the traditional bulk MIPs in rebinding target molecules based on the size, shape, and functionality. The specific structure associated with a flexible corona make MIPNs comparable with enzymes.[3] In addition, hydrolysis of the PtBMA shell will make these nanospheres water dispersible and be able to penetrate through cell membranes.[8] All these will make MIPNs promising candidates for sensing and bioapplications.

**Acknowledgment.** This work was supported by a grant (No. 0120RD) from the CRTI program. The authors are grateful to Dashan Wang for carrying out TEM experiments and Gilles Robertson for helpful $^1$H NMR discussions.

## References and Notes

(1) (a) Wulff, G. *Chem. Rev.* **2002**, *102*, 1. (b) Vlatakis, G. L.; Andersson, I.; Mosbach, K. *Nature (London)* **1993**, *361*, 645. (c) Zimmerman, S. C.; Lemcoff, N. G. *Chem. Commun.* **2004**, 5. (d) Batra, D. Shea, K. J. *Curr. Opin. Chem. Biol.* **2003**, *7*, 434. (e) Ye, L.; Haupt, K. *Anal. Bioanal. Chem.* **2004**, *378*, 1887.

(2) (a) Ye, L.; Weiss, R.; Mosbach, K. *Macromolecules* **2000**, *33*, 8239. (b) Yilmaz, E.; Ramström, O.; Möller, P.; Sanchez, D.; Mosbach, K. *J. Mater. Chem.* **2002**, *12*, 1577. (c) Carter, S. R.; Rimmer, S. *Adv. Mater.* **2002**, *14*, 667. (d) Wang, J.; Cormack, P. A. G.; Sherrington, D. C.; Khoshdel, E. *Angew. Chem., Int. Ed.* **2003**, *42*, 5336. (e) Ki, C. D.; Oh, C.; Oh, S.; Chang, J. Y. *J. Am. Chem. Soc.* **2002**, *124*, 14838.

(3) (a) Maddock, S. C.; Pasetto, P.; Resimini, M. *Chem. Commun.* **2004**, 536. (b) Biffis, A.; Graham, N. B. Siedlaczek, G.; Stalberg, S.; Wulff, G. *Macromol. Chem. Phys.* **2001**, *202*, 163.

(4) (a) Zimmerman, S. C.; Zharov, I.; Wendland, M. S.; Rakow, N. A.; Suslick, K. S. *J. Am. Chem. Soc.* **2003**, *125*, 13504. (b) Mertz, E.; Zimmerman, S. C. *J. Am. Chem. Soc.* **2003**, *125*, 3424.

(5) (a) Yang, H.; Zhang, S.; Yang,; Chen, W. X.; Zhuang, Z.; Xu, J.; Wang, X.; *J. Am. Chem. Soc.* **2004**, *126*, 4054. (b) Yang, H.; Zhang, S.; Tan, F.; Zhuang, Z.; Wang, X. *J. Am. Chem. Soc.* **2005**, *127*, 1378.

(6) Li, Z.; Day, M.; Ding, J.; Faid, K. *Macromolecules* **2005**, *38*, 2620.

(7) (a) Won, Y.; Davis, T.; Bates, F. S. *Science* **1999**, *283*, 960 (b) Zhang, L.; Yu, K.; Eisenberg, A. *Science* **1996**, *272*, 1777 (c) Li, Z.; Kesselman, E.; Talmon, Y.; Hillmyer, M. A.; Lodge, T. P. *Science* **2004**, *306*, 98. (d) Chen, Z.; Cui, H.; Hales, K.; Li, Z.; Qi, K.; Pochan, D. J.; Wooley, K. L. *J. Am. Chem. Soc.* **2005**, *127*, 8592. (e) Li, Z.; Liu, G.; Law, S.-J.; Sells, T. *Biomacromolecule* **2002**, *3*, 984. (f) Li, Z.; Liu, G. *Langmuir* **2003**, *19*, 10480.

(8) (a) Bronich, T. K.; Keifer, P. A.; Shlyakhtenko, L. S.; Kabanov, A. V. *J. Am. Chem. Soc.* **2005**, *127*, 8236. (b) Savic, R.; Luo, L.; Eisenberg, A.; Maysinger, D. *Science* **2003**, *300*, 615.

(9) (a) Duffy, D. J.; Das, K.; Hsu, S. L.; Penelle, J.; Rotello, V. M.; Stidham, H. D. *J. Am. Chem. Soc.* **2002**, *124*, 8290. (b) Hamilton, A. D.; Engen, D. V. *J. Am. Chem. Soc.* **1987**, *109*, 5035. (c) Stubbs, L. P.; Weck, M. *Chem.—Eur. J.* **2003**, *9*, 992. (d) Li, Z.; Ding, J.; Robertson, G.; Day, M.; Tao, Y. *Tetrahedron Lett.* **2005**, *46*, 6499.

CDV

(10) (a) Kugimiya, A.; Mukawa, T.; Takeuchi, T. *Analyst* **2001**, *126*, 772. (b) Kubo, H.; Nariai, H.; Takeuchi, T. *Chem. Commun.* **2003**, *2792*. (c) Manesiotis, P.; Hall, A. J.; Sellergren, B. *J. Org. Chem.* **2005**, *70*, 2729. (d) Manesiotis, P.; Hall, A. J.; Courtois, J.; Irgum,; Sellergren, K. B. *Angew. Chem., Int. Ed.* **2005**, *44*, 3902.
(11) Bernstein, J.; Stearns, B.; Shaw, E.; Lott, W. A. *J. Am. Chem. Soc.* **1947**, *69*, 1151−1158.
(12) Matyjaszewski, K.; Xia, J. *Chem. Rev.* **2001**, *101*, 2921.
(13) Zhang, L.; Eisenberg, A. *Macromolecules* **1999**, *32*, 2239.
(14) Ma, Y.; Kolotuchin, S. V.; Zimmerman, S. C. *J. Am. Chem. Soc.* **2002**, *124*, 13757.
(15) Zhou, J.; Li, Z.; Liu, G. *Macromolecules* **2002**, *35*, 3690.
(16) Bronstein, L. M.; Kostylev, M.; Tsvetkova, I.; Tomaszewski, J.; Stein, B.; Makhaeva, E. E.; Okhapkin, I.; Khokhlov, A. R. *Langmuir* **2005**, *21*, 2652.
(17) (a) Rampey, A. M.; Umpleby, R. J.; Rushton, G. T.; Iseman, J. C.; Shah, R. N.; Shimizu, K. D. *Anal. Chem.* **2004**, *76*, 1123. (b) Umpleby, R. J.; Baxter, S. C.; Chen, Y.; Shah, R. N.; Shimizu, K. D. *Anal. Chem.* **2001**, *73*, 4584.

MA0526793